

Delivery of Antibody-Like Molecules, Monobodies, Capable of Binding with SARS-CoV-2 Virus Nucleocapsid Protein, into Target Cells

Y. V. Khramtsov^a, A. V. Ulasov^a, T. N. Lupanova^a, Academician G. P. Georgiev^a,
and Corresponding Member of the RAS A. S. Sobolev^{a,b,*}

Received June 15, 2022; revised July 7, 2022; accepted July 11, 2022

Abstract—Based on previous studies, two antibody-like molecules, monobodies, capable of high-affinity interaction with the SARS-CoV-2 nucleocapsid protein (dissociation constant of tens of nM) were selected. For delivery to target cells, genetically engineered constructs containing monobody and TAT peptide, placed either at the N- or C-terminus of the resulting polypeptide, were produced and expressed in *E. coli*. The construct with the highest affinity to the SARS-CoV-2 nucleocapsid protein was revealed with the use of thermophoresis technique. Cellular thermal shift assay demonstrated the ability of this construct to interact with the nucleocapsid protein within HEK293T cells transfected with the SARS-CoV-2 nucleocapsid protein fused to the mRuby3 fluorescent protein. Replacement of TAT peptide to S10 shuttle peptide, containing endosomolytic peptide, significantly improved the penetration of the construct into the target cells.

Keywords: SARS-CoV-2, TAT peptide, S10 shuttle peptide, nucleocapsid protein, antibody-like molecules, monobody, thermophoresis, cellular thermal shift assay

DOI: 10.1134/S1607672922050088

The need to develop new antiviral drugs has become clearer than ever against the backdrop of the SARS-CoV-2 coronavirus pandemic. Along with the classical low-molecular-weight inhibitors of viral activity [1], it seems very promising to use antiviral drugs containing antibodies or antibody-like molecules that can be obtained for almost any protein antigen. In this regard, antibody-like molecules may be more promising due to their relatively small size compared to natural antibodies, while retaining the desired specificity and affinity [2]. One of the viral proteins that are critical for the assembly of the virus can be selected as a target. For the SARS-CoV-2 virus, this protein can be the nucleocapsid protein, or the N protein, which binds to viral RNA and takes an active part in the assembly and packaging of the virus and also has a number of other important functions for the virus [3–5]. In our previous work [6], we showed that several antibody-like molecules, monobodies (Fn-N), to the SARS-CoV N protein, created on the basis of the tenth domain of human type 3 fibronectin [7], are able to interact with high affinity with the N protein of the SARS-CoV-2 virus. For nonspecific delivery of these monobodies into cells, a cell-penetrating peptide can

be attached to them (for example, the TAT peptide, a peptide from the HIV-1 transcription transactivator protein) [8]. This was done for two monobodies Fn-N15 and Fn-N20, with the TAT peptide being located at the N- or C-terminus of the construct. The construct with the highest affinity for the N protein was selected from the obtained constructs. Next, the ability of this construct to bind to the N protein in HEK-293T cells was studied. To improve the efficiency of penetration into cells, a construct containing the shuttle peptide S10 instead of the TAT peptide was also studied [9].

Using genetic engineering methods, we obtained four plasmids, each of which contained a gene encoding an antibody-like molecule with a His tag and a TAT peptide at the N- or C-terminus. Plasmids encoding SARS-CoV-2 N protein with His-tag and SARS-CoV-2 N protein fused to the mRuby3 fluorescent protein were kindly provided by ShineGene company (China) and Dr. Raphael Gaudin (Addgene plasmid no. 170466), respectively. The antibody-like molecules fused with the TAT peptide and N protein were expressed in *E. coli* strain BL21(DE3). The expression of Fn-N with TAT and N protein was induced with 500 μ M IPTG for 20 h at 37°C for Fn-N with TAT and for 3 h at 37°C for N protein. Fn-N with TAT and N protein were isolated from the insoluble fraction [10] and then purified by affinity chromatography on columns packed with HisTrap FF for Fn-N with TAT and Protino® Ni-TED Resin for N protein.

^a Institute of Gene Biology, Russian Academy of Sciences, Moscow, Russia

^b Moscow State University, Moscow, Russia

*e-mail: alsobolev@yandex.ru

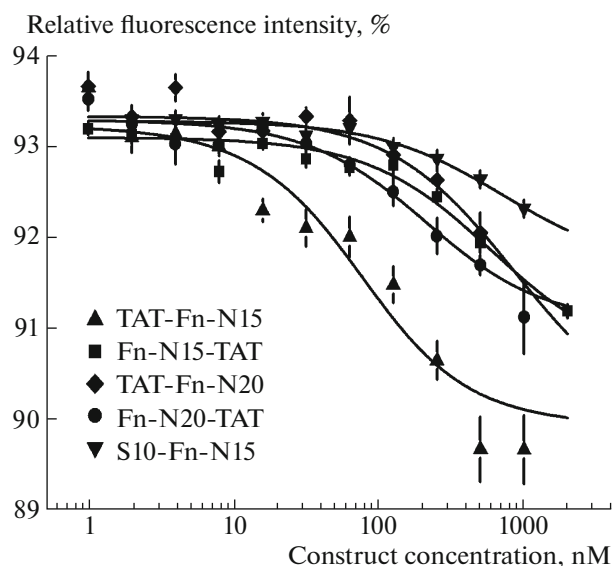


Fig. 1. Dependences of relative fluorescence intensities (fluorescence intensity before the start of thermophoresis is taken as 100%) 20 s after the start of thermophoresis on the concentration of polypeptide constructs at a constant concentration of the N protein (40 nM). Standard errors (SE) of relative fluorescence intensities are shown (8–12 replicates).

The isolated proteins were stored in a buffer containing 10 mM HEPES and 150 mM NaCl (pH 8).

Denaturing polyacrylamide gel electrophoresis demonstrated a sufficient degree of purity of the obtained proteins (98.9% for N protein, 98.8% for TAT-Fn-N15, 96% for Fn-N15-TAT, 61.5% for TAT-Fn-N20, 97.5% for Fn-N20-TAT, and 94.4% for S10-Fn-N15).

The interaction of the obtained polypeptide constructs with the N protein was studied as described in [6] by thermophoresis on a Monolith NT.115 Series instrument (NanoTemper Technologies GmbH, Germany) in a buffer containing 10 mM HEPES and 150 mM NaCl (pH 7). The N protein was labeled with the AF488 fluorescent dye as described in [6]. The degree of modification was 2.2 AF488 molecules per one N protein molecule. Cellular thermal shift analysis was performed on HEK293T cells transiently transfected with the N protein fused to the mRuby3 fluorescent protein as described in [11], except that the fluorescence of the samples was measured in capillaries on a Monolith NT.115 Series instrument (NanoTemper Technologies GmbH, Germany). For each polypeptide concentration, the sample was divided into four aliquots. The number of cells in aliquots and the percentage of transfection with the N protein (20–30%) fused with the red protein were determined using a MACSQuant Analyzer flow cytometer (Miltenyi Biotec, France). One aliquot was not heated, and the other three aliquots were heated to temperatures of 45, 50, and 55°C, respectively, for 3 min. Then, cell aliquots were lysed by four cycles of freezing in liquid nitrogen and thawing at 37°C. To separate from cell

debris and denatured proteins, the lysed cells were centrifuged at 8000 g for 1 h. The fluorescence of the buffer was subtracted from the fluorescence of each of the supernatants, and the resulting difference was normalized to the number of cells in the sample. The background value obtained for HEK293T cells not transformed with the N protein was subtracted from this normalized fluorescence. The obtained fluorescence value was normalized to the fluorescence of samples that were not subjected to heating.

At a fixed concentration of N-AF488 (40 nM), we used thermophoresis to obtain the dependences of relative fluorescence (fluorescence before thermophoresis was taken as 100%) 20 s after the start of thermophoresis on the concentration of the obtained constructs (Fig. 1). Four such dependences were obtained for each experiment, and the whole experiment was repeated two or three times. For each curve, the dissociation constant of the complex of the polypeptide construct with the N protein was determined. It was averaged over all 8–12 curves, and the relative measurement error was determined. The dissociation constants of the complexes of constructs with the N protein were 46 ± 5 , 710 ± 260 , 350 ± 80 , and 190 ± 90 nM for constructs TAT-Fn-N15, Fn-N15-TAT, TAT-Fn-N20, and Fn-N20-TAT, respectively. Thus, the best affinity for the N protein is observed for the TAT-Fn-N15 construct. For the S10-Fn-N15 construct (Fig. 1), the dissociation constant with the N protein was 700 ± 270 nM.

To study the interaction of the obtained constructs with the N protein in the cell, a variant of cellular thermal shift analysis in which the concentration of the added polypeptide construct changes was used [12]. Such dependences were obtained for the constructs TAT-Fn-N15 and S10-Fn-N15 on HEK293T cells at different temperatures, e.g., at 50°C (Fig. 2a). Interpolation of the sigmoid curve makes it possible to determine the amplitude of the transition, Δ_f , as well as to determine the proportion of the complex of the construct with the N protein at the selected temperature, Δ/Δ_f , at any concentration of the construct (Fig. 2a). This fraction can be extrapolated with a linear relationship to a temperature of 37°C (Fig. 2b) and, thereby, obtain the dependences of the proportion of the complex of the construct with the N protein on the concentration of the construct outside the cells at physiological temperatures (Fig. 2c). For the TAT-Fn-N15 and S10-Fn-N15 constructs, using the obtained curves, it was found that $EC_{50} = 10.1 \pm 0.8$ and 3.5 ± 0.8 μ M, respectively (Fig. 2c).

Thus, out of the four constructs obtained (two monobodies and the TAT peptide at the N or C terminus), the TAT-Fn-N15 construct has the highest affinity for the N protein of the SARS-CoV2 virus (dissociation constant 46 ± 5 nM). Cellular thermal shift analysis showed that this construct can penetrate HEK293T cells and interact in them with the N pro-

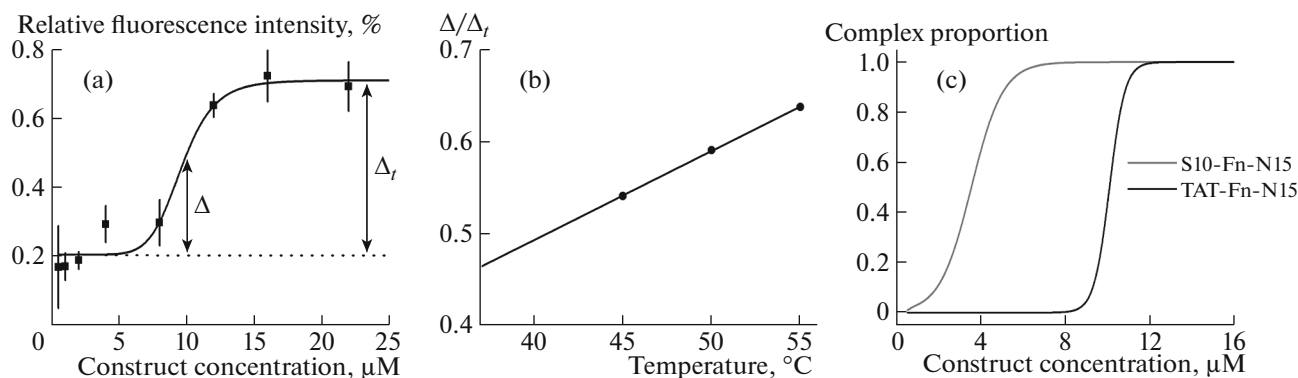


Fig. 2. (a) Dependence of relative fluorescence intensities (relative to the fluorescence intensity of the sample not subjected to heating) on the concentration of TAT-Fn-N15 construct obtained by heating for 3 min at 50°C. The data were interpolated with a sigmoid regression curve. (b) Temperature dependence of the ratio of the proportion of the TAT-Fn-N15 complex with the N protein (Δ) to the transition amplitude (Δ_T) at 10 μ M TAT-Fn-N15. The straight line shows the extrapolation of the experimental data to 37°C. (c) Dependences of the proportion of the S10-Fn-N15 or TAT-Fn-N15 complexes with the N protein on the concentration of the construct outside the cells under physiological conditions.

tein fused to the mRuby3 fluorescent protein. The inclusion of the S10 shuttle peptide [9], which contains both the improved TAT peptide and the endosomolytic peptide, instead of the TAT peptide, leads to a threefold decrease in EC_{50} (Fig. 2c). Despite the fact that the affinity of the S10-Fn-N15 construct for the N protein is 15 times lower than the affinity of the TAT-Fn-N15 construct, this is well compensated by the increase in the efficiency of penetration of the construct with S10 compared to the construct with the TAT peptide into cells. It should be noted that, previously, the S10 shuttle peptide was added simultaneously with the delivered construct; i.e., they did not form a chemical bond with each other [9]. In the present study, it was shown that the S10 is also effective in fused constructs. However, in the resulting construct, S10 significantly decreases the affinity of the monobody for the N protein. The effectiveness of the construct can be further increased by increasing this affinity, for example, by inserting an additional spacer between the S10 and the monobody, or by choosing a different monobody.

As a result of this study, we demonstrated that the S10-Fn-N15 construct has the highest efficiency of interaction with the N protein of the SARS-CoV-2 virus in HEK293T cells. This construct can potentially become the basis of an antiviral drug targeting both SARS-CoV and SARS-CoV-2.

ACKNOWLEDGMENTS

The experiments were carried out using the equipment of the Core Facility of the Institute of Gene Biology, Russian Academy of Sciences.

FUNDING

The study was supported by the Russian Science Foundation (project no. 21-14-00130).

COMPLIANCE WITH ETHICAL STANDARDS

The authors declare that they have no conflicts of interest. This article does not contain any studies involving animals or human participants performed by any of the authors.

REFERENCES

1. Clercq, E.D. and Li, G., *Clin. Microbiol. Rev.*, 2016, vol. 29, pp. 695–747.
2. Gebauer, M. and Skerra, A., *Annu. Rev. Pharmacol. Toxicol.*, 2020, vol. 60, pp. 391–415.
3. Surjit, M. and Lal, S.K., *Infect. Genet. Evol.*, 2008, vol. 8, pp. 397–405.
4. Wu, C. and Zheng, M., Preprints, 2020, p. 2020020247.
5. Prajapat, M., Sarma, P., Shekhar, N., et al., *Indian J. Pharmacol.*, 2020, vol. 52, p. 56.
6. Khrantsov, Y.V., Ulasov, A.V., Lupanova, T.N., et al., *Dokl. Biochem. Biophys.*, 2022, vol. 503, pp. 90–92.
7. Liao, H.-I., Olson, C.A., Hwang, S., et al., *J. Biol. Chem.*, 2009, vol. 284, pp. 17512–17520.
8. Reis, L.G. and Traini, D., *Expert Opin. Drug Deliv.*, 2020, vol. 17, pp. 647–664.
9. Krishnamurthy, S., Wohlford-Lenane, C., Kandimala, S., et al., *Nat. Commun.*, 2019, vol. 10, p. 4906.
10. Li, G., Li, W., Fang, X., et al., *Protein Expr. Purif.*, 2021, vol. 186. <https://doi.org/10.1016/j.pep.2021.105908>
11. Naidu, S.D., Dikovskaya, D., Moore, T.W., et al., *STAR Protocols*, 2022, vol. 3, p. 101265.
12. Molina, D.M., Jafari, R., Ignatushchenko, M., et al., *Science*, 2013, vol. 341, pp. 84–87.

Translated by M. Batrukova